

# Methylation of Zebularine Investigated Using Density Functional Theory Calculations

LALITHA SELVAM, FANG FANG CHEN, FENG WANG

*Environment and Biotechnology Centre, Faculty of Life and Social Sciences, Swinburne University of Technology, Hawthorn, Melbourne, Victoria 3122 Australia*

*Received 2 July 2010; Revised 1 December 2010; Accepted 10 February 2011*

*DOI 10.1002/jcc.21785*

*Published online 3 May 2011 in Wiley Online Library (wileyonlinelibrary.com).*

**Abstract:** Deoxyribonucleic acid (DNA) methylation is an epigenetic phenomenon, which adds methyl groups into DNA. This study reveals methylation of a nucleoside antibiotic drug 1-( $\beta$ -D-ribofuranosyl)-2-pyrimidinone (zebularine or zeb) with respect to its methylated analog, 1-( $\beta$ -D-ribofuranosyl)-5-methyl-2-pyrimidinone (d5) using density functional theory calculations in valence electronic space. Very similar infrared spectra suggest that zeb and d5 do not differ by types of the chemical bonds, but distinctly different Raman spectra of the nucleoside pair reveal that the impact caused by methylation of zeb can be significant. Further valence orbital-based information details on valence electronic structural changes caused by methylation of zebularine. Frontier orbitals in momentum space and position space of the molecules respond differently to methylation. Based on the additional methyl electron density concentration in d5, orbitals affected by the methyl moiety are classified into primary and secondary contributors. Primary methyl contributions include MO8 (57a), MO18 (47a), and MO37 (28a) of d5, which concentrates on methyl and the base moieties, suggest certain connection to their Frontier orbitals. The primary and secondary methyl affected orbitals provide useful information on chemical bonding mechanism of the methylation in zebularine.

© 2011 Wiley Periodicals, Inc. J Comput Chem 32: 2077–2083, 2011

**Key words:** methylation; zebularine; d5; DFT calculations; infrared spectra; Raman spectra; valence ionization energies

## Introduction

Deoxyribonucleic acid (DNA) methylation is an epigenetic phenomenon, which adds methyl groups into DNA, thereby influences gene expression, mutagenesis, carcinogenesis, and other processes.<sup>1,2</sup> Most studies in Nature Neuroscience suggested that the adult brain utilizes DNA methylation to preserve long-lasting memories,<sup>3</sup> as a behavioral memory's lifetime represents multiple molecular lifetimes, which DNA methylation is one of the candidate in the necessity for a self-perpetuating signal.<sup>3</sup> Another recent study revealed that patients diagnosed with brain tumors or gliomas with a certain, stable pattern of hypermethylation (glioma-CpG island methylator phenotype; G-CIMP) have better clinical outcomes than patients who do not have the mods.<sup>4</sup> On the other hand, many nucleoside analogs form an important class of anti-cancer<sup>5</sup> and anti-AIDS<sup>6</sup> drugs have been identified as potential agents to reverse the effects of methylation. For example, 1-( $\beta$ -D-ribofuranosyl)-2-pyrimidinone (zebularine or zeb) and its methylated product 1-( $\beta$ -D-ribofuranosyl)-5-methyl-2-pyrimidinone (d5), which are both pyrimidine analogs, have been reported as inhibitors of DNA methyltransferases<sup>7</sup> and cytidine deaminases.<sup>8</sup> Structurally, d5 is a product

when a hydrogen atom at the C(5) position in zeb is replaced by a methyl (CH<sub>3</sub>) group.

Structural investigation of nucleosides and nucleotides has been of major interest for many years,<sup>9–14</sup> as such information adds to our understanding of biochemical and biophysical processes of DNA/RNA, such as methylation,<sup>15</sup> alkylation,<sup>16,17</sup> and photoionization.<sup>18</sup> Molecular spectra are largely dependent on local structures and their chemical environment.<sup>19</sup> Electronic structures are particularly important to understand their molecular properties and interactions, in which spectroscopy plays an important role. For example, infrared (IR) and Raman spectroscopic techniques are useful to identify functional groups such as the extra methyl group of d5, hereby to probe the methylation impact of zeb. IR spectra are also useful to probe interactions such as hydrogen bond caused improper blue shift.<sup>20</sup> Very

Additional Supporting Information may be found in the online version of this article.

**Correspondence to:** F. Wang; e-mail: fwang@swin.edu.au

Contract/grant sponsor: National Computational Infrastructure (NCI); Merit Allocation Scheme at ANU

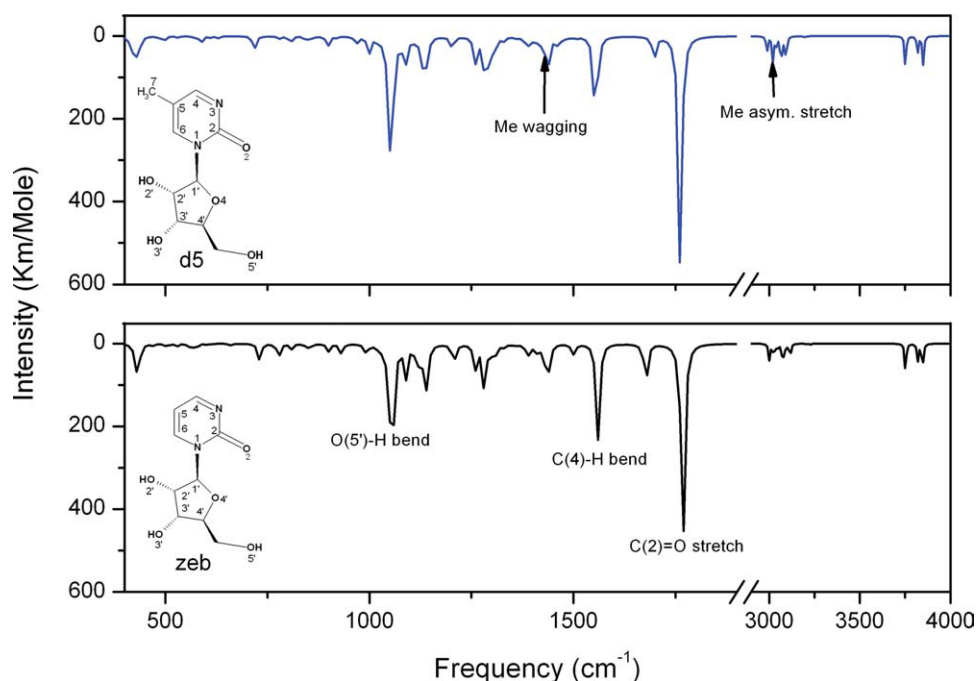


**Figure 1.** Comparison of simulated infrared (IR) spectra of d5 (upper panel) and zeb (lower panel). The IR spectra exhibit similarities of zeb and d5. [Color figure can be viewed in the online issue, which is available at [wileyonlinelibrary.com](http://wileyonlinelibrary.com).]

recently, IR spectra have been used to study different intramolecular hydrogen bonds in conformers of zidovudine,<sup>21</sup> a nucleoside anti-HIV drug. On the other hand, photoelectron spectroscopy and electron momentum spectroscopy (EMS) have been proven useful techniques to study orbital based electronic structures of molecules. A recent review given by Takahashi and their applications to biomolecules has been documented.<sup>22,23</sup> Combining the spectroscopic means to investigate methylation of zeb is able to provide a more comprehensive understanding of the important processes in nucleosides. In the present study, we reveal the methylation process from a combined spectroscopic method and from orbital based information in momentum space.

## Methods and Computational Details

IR and Raman spectra of zeb and d5 are simulated on the optimized structure using the B3LYP/cc-pVTZ model. The basis set used for single point calculations is Dunning's augmented correlation corrected triple zeta plus polarization (aug-cc-pVTZ).<sup>24</sup> In the recent assessment performance of DFT methods and basis sets, it is found that when combined with B3LYP, this model (B3LYP/aug-cc-pVTZ) exhibits a general excellent performance and in particular to mimic the experimental EMS of small molecules such as water<sup>25</sup> and nitric oxide. Computational chemistry packages such as GAUSSIAN03<sup>26</sup> and GAMESS<sup>27</sup> are used. The orbital wavefunctions obtained from position space were transformed into orbital momentum profiles through a Fourier transformation, under certain approximations such as independ-

ent particle approximation and plane wave impulse approximation.<sup>28</sup> The theoretical orbital momentum distributions of the species are produced using a modified NEMS code.<sup>29</sup>

Following our lead in the development of 3D-PDF graphic presentation of interactive three-dimensional (3D) structures (online or on a computer),<sup>30</sup> we extend the interactive 3D-PDF technique to exhibit vibration animation, which associates Raman spectral peak for methyl vibration using the same technique.

## Results and Discussion

### Vibrational Spectroscopy

Vibrational spectroscopy is a useful tool to identify a particular fragment in a molecule and interactions. IR and Raman activities are in complement, which can be used to characterize the vibrational states of molecules. Figure 1 compares the simulated IR spectra of the nucleoside pair zeb and d5 (the major spectral peaks are assigned in the figure). IR spectrum identifies compounds and composition. Zeb and d5 possess very similar structures with the same compositions, for example, C=O, C—H, and O—H, so that only subtle differences between the nucleoside pair are shown in the IR spectra. The methyl related vibrations belong to a number of C—H related vibrations in the IR spectrum of d5. As a result, IR spectra of zeb and d5 indicate their structural similarities.

Raman spectra yields complementary information to the IR spectra of molecules. We, therefore, simulated Raman spectra of the nucleoside pair to explore methyl responses in d5 with respect to zeb. Figure 2 reports the Raman spectra of zeb and d5

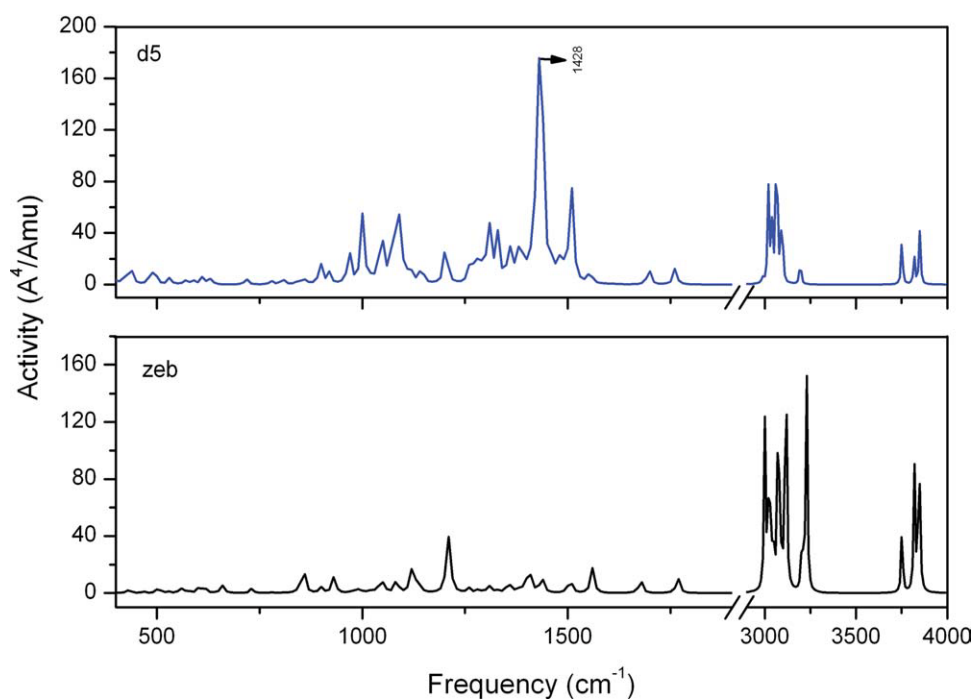


**Figure 2.** Simulated Raman spectra of zeb and d5. Double click on the 3D structure of d5 for its methyl bending vibration. The Raman spectra demonstrate methyl impact in d5 structure.

and they indeed show apparent differences between the molecules caused by methylation. For example, the spectrum of d5 (upper panel) are significantly enhanced in the region of 700–1500  $\text{cm}^{-1}$ , whereas in the region with  $>3000 \text{ cm}^{-1}$ , the zeb spectrum shows stronger vibrations. In particular, the spectral peak at  $1428 \text{ cm}^{-1}$  of d5 clearly indicates that this molecule engages with an extra functional group of atoms (i.e., methyl), which does not exist in zeb, that is, a methyl signature band as demonstrated in the embedded animated 3D vibrational mode. To view the methyl bending vibrational animation, click on the 3D structure to activate it.

The major spectral peak positions and intensities of the IR and Raman spectra of zeb and d5 are summarized in Table I for comparison. As seen that the major IR spectral peaks of zeb do not change apparently in either peak positions or intensities in d5, indicating that d5 and zeb contain the same bond types and the extra methyl ( $\text{CH}_3$ ) group in d5 does not introduce new types of chemical bonds to the existing ones in zeb. Only a small number of peaks exhibit noticeable differences in both frequencies and intensities, and the methyl effects could either enhance or discriminate the peaks. For example, the methyl group causes the enhancement and shift of an IR spectral peak of zeb at  $1128 \text{ cm}^{-1}$  apparently. The intensity of the spectral peak is enhanced from 29 to 138  $\text{Km/mol}$  and the frequency shifts  $14 \text{ cm}^{-1}$  to  $1134 \text{ cm}^{-1}$  in d5. In contrary with this enhancement, a spectral peak of zeb at  $1677 \text{ cm}^{-1}$  with an intensity of 100  $\text{Km/mol}$  is reduced to 58  $\text{Km/mol}$  and is shifted  $20 \text{ cm}^{-1}$  to  $1697 \text{ cm}^{-1}$  in d5.

The Raman spectra of the molecules show a clear trends of methyl enhancement ( $<2000 \text{ cm}^{-1}$ ) and discrimination

( $>3000 \text{ cm}^{-1}$ ) of the spectrum. Apart from the methyl signature peak at  $1428 \text{ cm}^{-1}$ , a large number of peaks in the region below  $2000 \text{ cm}^{-1}$  are also enhanced. For example, as given in Table 1, a Raman spectral peak of d5 at  $1284 \text{ cm}^{-1}$  with  $116 \text{ A}^4/\text{Amu}$  is hardly seen as the corresponding spectral peak in zeb at  $1280 \text{ cm}^{-1}$  with  $\sim 1 \text{ A}^4/\text{Amu}$  Raman activities.

#### *Ionization Potentials and Frontier Orbitals*

The methyl group activities of d5 stand out in its Raman spectrum with respect to zeb. The Raman spectra do not, however, tell us the impact of methyl group to the electronic structures of d5 with respect to zeb, that is, which orbitals are affected and how are they affected. For this reason, ionization potentials of the molecule pair are calculated using outer valence Green's function (OVGF)/triple zeta valence plus polarization (TZVP),<sup>31,32</sup> statistical average of orbital potential (SAOP)/et-pVQZ<sup>33</sup> and B3LYP/aug-cc-pVTZ and are given and compared in Table 2 (for the theoretical photoelectron spectra of zeb and d5, please see ref. 30). It is seen that valence ionization potentials produced by the OVGF/TZVP model agree with the SAOP/et-pVQZ model when the hole moves inwards. For large and near-nano sized nucleosides, such as zeb and d5, methylation is not a local effect as we have seen in small molecules such as glycine and L-alanine<sup>34</sup> but spread over the entire valence space. Nevertheless, based on the ionization energy differences (e.g., SAOP energies), valence orbitals of the nucleoside pair are classified as primary methyl dominant group of MO8(57a), MO18(47a), and MO37(28a) (orbitals only for d5; Marked bold in Table 2); secondary methyl affected orbitals such as HOMO(as MO1 which refers to 60a in zeb and

**Table 1.** Simulated Vibrational Frequencies ( $\nu$ ,  $\text{cm}^{-1}$ ), IR Intensities (Km/mol), and Raman Activities ( $\text{A}^4/\text{Amu}$ ) of Major Peaks for Zeb and d5<sup>a</sup>.

zeb					d5			
Mode No.	$\nu$ ( $\text{cm}^{-1}$ )	IR (Km/mol)	Raman ( $\text{A}^4/\text{Amu}$ )	Assignment <sup>b</sup>	Mode No.	$\nu$ ( $\text{cm}^{-1}$ )	IR (Km/mol)	Raman ( $\text{A}^4/\text{Amu}$ )
78	3846	68	115	<i>sO(3')</i> —H	87	3849	69	41
77	3820	41	87	<i>sO(5')</i> —H	86	3818	40	21
76	3752	72	47	<i>sO(2')</i> —H	85	3751	76	35
75	3229	2	155	<i>asMe</i> (d5), <i>C(5)</i> —H (zeb)	83	3096	16	25
71	3076	39	81	<i>asC(5')</i> —H—H	80	3071	24	8
68	3024	32	107	<i>ssC(5')</i> —H—H	75	3020	43	62
67	3001	42	123	<i>sC(4')</i> —H	74	2987	39	4
66	1767	537	537	<i>sC=O</i>	73	1761	585	13
65	1677	100	10	<i>bC(6)</i> —H, <i>C(4)</i> —H, <i>C(5)</i> — <i>C(6)</i> + Me (d5)	72	1697	58	13
64	1559	232	17	<i>sC(4)</i> — <i>C(5)</i>	71	1554	239	10
60	1437	35	7	<i>bC(2')</i> —H, <i>C(3')</i> —H, <i>O(2')</i> —H+ Me (d5)	65	1436	28	97
<b>59</b>	<b>1427</b>	<b>42</b>	<b>2</b>	<b><i>bO2'</i>—(H), <i>O(3')</i>—H, <i>C(1')</i>—H, <i>C(2')</i>—H, <i>C(3')</i>—H, <i>C(4')</i>—H (zeb), <i>wagMe</i> (d5)</b>	<b>64</b>	<b>1428</b>	<b>1</b>	<b>140</b>
50			1	<i>bC(6)</i> —H, <i>C(3')</i> —H, <i>C(4')</i> —H, <i>C(1')</i> —H (zeb)	54	1284	120	116
	1280	100		<i>bC(4)</i> —H, <i>C(3')</i> H, <i>C(4')</i> —H, <i>C(1')</i> —H,+ Me (d5)				
44	1128	29	3	<i>b(C2')</i> —H, <i>sC(2')</i> — <i>O(2')</i>	48	1134	138	1
39	1055	347	1	<i>bC(5')</i> — <i>O(5')</i>	42	1053	389	8
38	1045	43	10	<i>bO(3')</i> —H, <i>C(2')</i> —H, <i>C(4')</i> —H (zeb), <i>bC(4')</i> —H (d5)	38	1000	3	44

<sup>a</sup>Based on the B3LYP/cc-pVTZ model.<sup>b</sup>Assigned vibrational mode abbreviations used in Table I: *s* stretch, *as* and *ss* are asymmetric and symmetric stretch, respectively, *b* for bend mode and Me for methyl.

64a in d5), MO13, MO21, MO27, MO34, MO36, and MO40 ( $|\Delta\text{IP}| \geq 0.20$  eV) and other orbitals with minor energy changes ( $|\Delta\text{IP}| < 0.20$  eV; refer to Supporting Information).

Accurate calculations of ionization energies for larger molecules have been always a challenge to theoreticians.<sup>22</sup> However, valence ionization spectra of molecules are usually more accessible than core ionization spectra, as smaller relaxation effects in valence space mean that even the Hartree–Fock orbital energies can be good approximations for ionization energies through the Koopman’s theorem. For smaller molecules such as benzene,<sup>35</sup> the sophisticated ADC(3) model,<sup>36</sup> is able to produce accurate ionization energies for the valence orbitals. However, for larger molecules, such as zebularine and d5, this ADC(3) model is restricted by computational resources. As a result, the OVGf model,<sup>31,32</sup> which solves the Dyson equation for the ionization energies of a molecule rather than using the negative values of the orbital energies to approximate the ionization energies as in the HF and DFT models using the Koopman’s theorem and “meta-Koopman’s theorem,”<sup>37</sup> respectively, is able to produce more accurate results. However, the OVGf model only applies to the outer valence region of usually  $\varepsilon < 20$  eV. If one needs to estimate ionization energies for molecules at the size of Zeb or d5, the SAOP model<sup>33</sup> is able to produce accurate estimations, whereas the orbital energies of B3LYP does not represent the correct ionization energies. As a result, some experiments use a nonphysically meaningful simple average of orbitals energies from HF and B3LYP, simply because that the former (HF)

overestimates but the latter (B3LYP) underestimates the ionization energies.<sup>38</sup>

Chemical properties and reactions are dominated by valence electronic structures of a molecule, such as Frontier orbitals including the highest occupied molecular orbital (HOMO), the next HOMO (NHOMO), the third HOMO (THOMO), and so on. The IP differences between the HOMOs of d5 and zeb are larger than those in NHOMOs and THOMOs, that is,  $-0.24$ ,  $-0.10$ , and  $-0.09$  eV (based on SAOP/TZVP model), respectively. However, the orbitals can hardly be compared quantitatively as they are presented as density distributions, which brings significant challenges when the orbital differences are subtle. Orbitals in momentum space when combined with orbital electron density are able to achieve this goal, which is also called dual space analysis (DSA).<sup>39</sup> Figure 3 depicts theoretical orbital momentum distributions and electron density distributions of the HOMO, NHOMO, and THOMO of zeb and d5, accordingly. The three Frontier orbitals of zeb and d5 reveal very different bonding characters, as demonstrated in the orbital electron densities (orbital in position space in Fig. 3). For example, the HOMOs are concentrated on the base moiety of the nucleosides. In the NHOMOs, the electron density is in a transition to spread across the base moiety into the sugar moiety through the glycosyl bond, whereas in the THOMOs, the orbital electron density spreads all over the nucleosides, base, and sugar.

From position space information (i.e., the energies and orbitals), it is obvious that the differences are caused by methylation

**Table 2.** Comparison of Valence Orbital Ionization Energies (eV) of Zeb and d5 Calculated Using Different Models<sup>a,b</sup>.

MO	zeb				d5			
	Orbital	OVGF/TZVP	SAOP/et-pVQZ	B3LYP/aug-cc-pVTZ	Orbital	OVGF/TZVP	SAOP/et-pVQZ	B3LYP/aug-cc-pVTZ
HOMO–LUMO gap		<u>6.47</u>	<u>3.35</u>	<u>4.73</u>		<u>6.15</u>	<u>3.20</u>	<u>4.56</u>
<u>1 (HOMO)</u>	<u>60a</u>	<u>8.41</u>	<u>10.35</u>	<u>6.69</u>	<u>64a</u>	<u>8.12</u>	<u>10.11</u>	<u>6.37</u>
2	59a	9.67	10.60	7.30	63a	9.56	10.50	7.12
3	58a	10.04	10.80	7.48	62a	9.97	10.71	7.32
4	57a	10.56	11.21	7.90	61a	10.47	11.12	7.73
5	56a	10.79	11.46	8.19	60a	10.85	11.40	8.06
6	55a	11.27	11.95	8.67	59a	11.06	11.86	8.51
7	54a	11.67	12.29	9.02	58a	11.52	12.22	8.88
<b>8</b>					<b><u>57a</u></b>	<b><u>11.84</u></b>	<b><u>12.57</u></b>	<b><u>9.14</u></b>
9	53a	12.10	12.75	9.40	56a	12.00	12.73	9.45
10	52a	12.08	12.79	9.60	55a	12.37	12.88	9.54
11	51a	12.42	13.15	9.89	54a	13.11	13.25	10.02
12	50a	13.20	13.36	10.18	53a	13.30	13.46	10.25
<u>13</u>	<u>49a</u>	<u>13.37</u>	<u>13.56</u>	<u>10.41</u>	<u>52a</u>	<u>13.49</u>	<u>13.75</u>	<u>10.60</u>
14	48a	13.75	13.93	10.78	51a	13.88	13.95	10.82
15	47a	13.97	14.16	11.17	50a	13.95	14.23	11.19
16	46a	14.50	14.58	11.53	49a	14.43	14.48	11.35
17	45a	14.55	14.78	11.80	48a	14.49	14.66	11.56
<b>18</b>					<b><u>47a</u></b>	<b><u>14.67</u></b>	<b><u>14.70</u></b>	<b><u>11.63</u></b>
19	44a	14.81	14.86	11.92	46a	14.86	14.76	11.73
20	43a	14.86	15.14	12.10	45a	14.81	15.04	12.04
<u>21</u>	<u>42a</u>	<u>15.17</u>	<u>15.41</u>	<u>12.48</u>	<u>44a</u>	<u>14.83</u>	<u>15.18</u>	<u>12.10</u>
22	41a	15.65	15.70	12.77	43a	15.32	15.55	12.53
23	40a	15.68	15.95	12.98	42a	15.67	15.88	12.84
24	39a	16.23	16.20	13.27	41a	16.16	16.12	13.12
25	38a	16.28	16.29	13.42	40a	16.28	16.26	13.32
26	37a	16.58	16.64	13.75	39a	16.50	16.58	13.62
<u>27</u>	<u>36a</u>	<u>17.66</u>	<u>17.29</u>	<u>14.46</u>	<u>38a</u>	<u>17.21</u>	<u>17.03</u>	<u>14.11</u>
28	35a	17.73	17.68	14.82	37a	17.79	17.58	14.65
29	34a	18.03	17.77	15.04	36a		17.74	14.90
30	33a	18.09	18.11	15.31	35a		18.02	15.18
31	32a	18.91	18.53	15.78	34a		18.35	15.51
32	<u>31a</u>		<u>19.66</u>	<u>17.00</u>	33a		19.58	16.85
33	<u>30a</u>		<u>19.91</u>	<u>17.23</u>	32a		19.76	17.02
<u>34</u>	<u>29a</u>		<u>20.48</u>	<u>17.90</u>	<u>31a</u>		<u>20.19</u>	<u>17.48</u>
35	28a		21.12	18.58	30a		20.96	18.34
<u>36</u>	<u>27a</u>		<u>21.87</u>	<u>19.37</u>	<u>29a</u>		<u>21.61</u>	<u>19.03</u>
<b>37</b>					<b><u>28a</u></b>		<b><u>22.15</u></b>	<b><u>19.61</u></b>

<sup>a</sup>Primary methyl orbitals are bold and methyl affected orbitals are underlined.

<sup>b</sup>Only the lowest orbitals with  $\epsilon_i \leq 15.50$  eV are listed here (see the Supporting Information for the complete valence energies).

between zeb and d5, except that the methyl group is populated in the HOMO of d5. However, the orbitals in momentum space clearly differentiate such subtle differences between the three pairs of very similar orbitals of zeb and d5, as exhibited in Figure 3. Although the HOMOs of the nucleoside pair look very similar, the methyl group in d5 is indeed populated, which contributes to the shift of MDs in small momentum region. It is even more difficult to differentiate the NHOMOs and THOMOs in the molecule pair by their densities, but achievable in their orbitals in momentum space. For example, the NHOMOs pair, that is, 59a (zeb) and 63a (d5), in Figure 3 show that the lower

momentum region ( $p < 0.5$  a.u) exhibits measurable differences. Unlike the HOMOs, the NHOMOs exhibit strong sp-hybrid nature with an antibonding nature. In addition, the NHOMOs are very similar except for opposite signs in zeb and d5, as the methyl moiety contributes little to this orbital (not well populated) in d5. The last outermost valence orbital pair is the third HOMOs (THOMOs, Fig. 3), which are the orbitals exhibiting strong interactions of the fragments and chemical bonding. Electron densities from both base and sugar moieties, that is, from the entire nucleosides, bond the base-sugar pair together in this orbital.

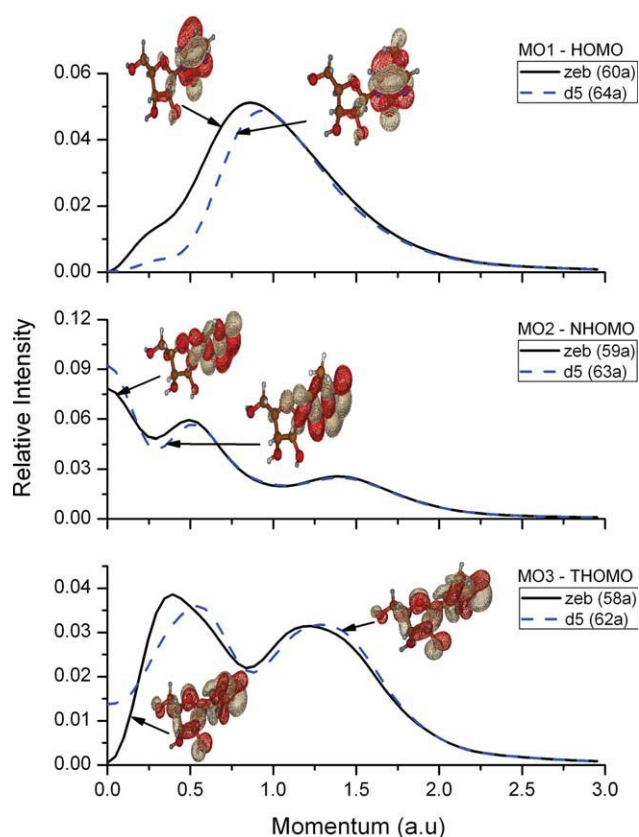


**Figure 3.** Momentum and electron density distributions of HOMO, NHOMO, and THOMO in the outer valence shell of zeb and d5 (3D structures can be provided upon request).

#### The Methyl Signature Valence Orbitals

Methylation effects are found to delocalize all over the valence region in zeb and d5, rather than being restricted into a group of identifiable orbitals in small molecules such as glycine and L-alanine.<sup>34</sup> However, methyl contributions in d5 can be approximately categorized into primary, secondary, and minor contributors. Primary contributors are signature orbitals of the methyl group in the valence space, namely, MO8 (57a), MO18 (47a), and MO37 (28a), which have been identified previously<sup>30</sup> by their ionization energies. Orbital momentum profiles of the primary methyl orbitals, along with their electron density distributions in position space are given in Figure 4.

All methyl signature orbitals concentrate on the base moiety of d5 as the methyl group is attached to the base. The orbitals show quite different densities in the sugar moiety although minor. The methyl signature orbitals 57a, 47a, and 28a are parallel to the Frontier orbitals (Fig. 3) in certain aspects. Like the Frontier orbitals of the nucleoside pair, the methyl signature orbitals exhibit varied chemical bonding characters as shown in their orbital profiles. For example, the lowest IP orbital of methyl signature in d5, MO8 (57a), which exhibits a character similar to the HOMO of d5, concentrates on the base moiety and is dominated by bell-shaped orbital profiles. The next methyl dominated orbital, MO18 (47a), shows a *sp*-hybrid nature. This orbital is also dominated by the base

moiety of d5, but small contribution in sugar along the N(1)–C(1′)–C(2′)–O(2′)–H chain is observed. The methyl group exhibits significantly different interactions in orbital 47a, in contrary to orbital 57a. The last methyl related orbital, MO37 (28a), which bonds the methyl, the base, and the sugar together along the C(7)–H–H–H–C(5)–C(6)–N(1)–C(1′)–C(2′)–C(3′) chain, can be clearly visualized from the orbital contour in Figure 4. As a result, the three methyl dominant orbitals reflect their unique methylation characters in d5.

#### Conclusions

Methylation of zebularine has been investigated using density functional theory with respect to d5. It is found that while the composition and chemical bond types of zeb and d5 are confirmed using IR spectra, it is Raman spectra which is able to identify the structural differences between zeb and d5 caused by methyl. However, only detailed orbital-based analysis is able to reveal the complex structures of the nucleoside pair, as properties and behavior of the methylation deeply root into their electronic structures. The present orbital-based electronic structural analysis shows similarities and differences in the Frontier orbitals, HOMO, NHOMO, and THOMO between zeb and d5, in response to methylation.

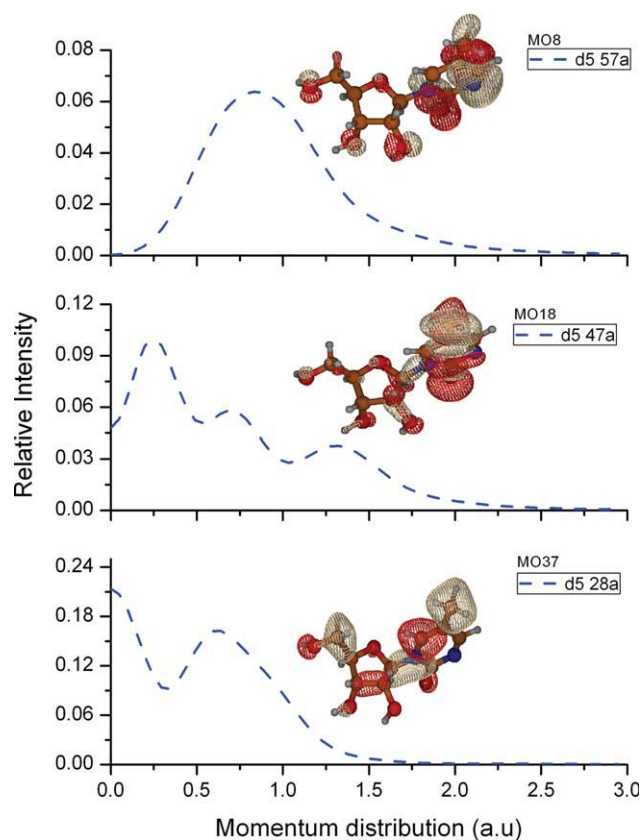


**Figure 4.** Momentum distributions and electron density distributions of the primary methyl orbitals MO8, MO18, and MO37 of d5 (3D structures can be provided upon request).

The responses of the valence electrons to the methylation is largely delocalized in such large and near-nanosized nucleosides, in contrary to more localized responses to methylation in small molecules such as L-alanine.<sup>34</sup> With the help of orbital electron density distributions and orbital momentum profiles, it is able to recognise methylation in d5 as methyl signature orbitals of 57a, 47a, and 28a, which are base-dominated orbitals. The present study provide useful information regarding individual valence orbitals to the methylation processes for nucleosides.

## Acknowledgments

LS acknowledges Swinburne University Postgraduate Research Award (SUPRA) and FC acknowledges the Postgraduate Research Award from the Faculty of ICT at Swinburne University of Technology. The authors thank Dr. C. G. Ning of Tsinghua University for assistance on the NEMS code.

## References

1. Wainfan, E.; Poirier, L. A. *Cancer Res* 1992, 52, 2071.
2. Newell-Price, J.; Clark, A.J.L.; King, P. *Trends Endocrinol Metabol* 2000, 11, 142.
3. Miller, C. A.; Gavin, C. F.; White, J. A.; Parrish, R. R.; Honasoge, A.; Yancey, C. R.; Rivera, I. M.; Rubio, M.D.; Rumbaugh, G.; Sweatt, J. D. *Nat Neurosci* 2010, 13, 664.
4. Noushmehr, H.; Weisenberger, D. J.; Diefes, K.; Phillips, H. S.; Pujara, K.; Berman, B. P.; Pan, F.; Pelloski, C. E.; Sulman, E. P.; Bhat, K. P.; Verhaak, R. G. W.; Hoadley, K.A.; Hayes, D. N.; Perou, C. M.; Schmidt, H. K.; Ding, L.; Wilson, R. K.; Van Den Berg, D.; Shen, H.; Bengtsson, H.; Neuvial, P.; Cope, L. M.; Buckley, J.; Herman, J. G.; Baylin, S. B.; Laird, P. W.; Aldape, K. *Cancer Cell* 2010, 17, 510.
5. Galmarini, C. M.; Jordheim, L.; Dumontet, C. *Expert Rev Anticancer Ther* 2003, 3, 717.
6. el Kouni, M. H. *Curr Pharm Des* 2002, 8, 581.
7. Zhou, L.; Cheng, X.; Connolly, B. A.; Dickman, M. J.; Hurd, P. J.; Hornby, D. P. *J Mol Biol* 2002, 321, 591.
8. Holy, A.; Ludzisa, A.; Votruba, I.; Sediva, K.; Pischel, H. *Collect Czech Chem Commun* 1985, 50, 393.
9. Tasaki, K.; Yang, X.; Urano, S.; Fetzer, S.; LeBreton, P. R. *J Am Chem Soc* 1990, 112, 538.
10. Wesolowski, S. S.; Leininger, M. L.; Pentchev, P. N.; Schaefer, H.F. *J Am Chem Soc* 2001, 123, 4023.
11. Lottermoser, U.; Rademacher, P.; Mazik, M.; Kowski, K. *Eur J Biochem* 2005, 3, 522.
12. Fonseca Guerra, C.; Bickelhaupt, F. M.; Saha, S.; Wang, F. *J Phys Chem A* 2006, 110, 4012.
13. Saha, S.; Wang, F.; Brunger, M. J. *Mol Simul* 2006, 32, 1261.
14. Thompson, A.; Saha, S.; Wang, F.; Tsuchimochi, T.; Nakata, A.; Imamura, Y.; Nakai, H. *Bull Chem Soc Jpn* 2009, 82, 187.
15. Rountree, M.R.; Bachman, K.E.; Herman, J.G.; Baylin, S.B. *Oncogene* 2001, 20, 3156.
16. Kim, N. S.; LeBreton, P. R. *J Am Chem Soc* 1996, 118, 3694.
17. Kim, N. S.; Zhu, Q.; LeBreton, P. R. *J Am Chem Soc* 1999, 121, 11516.
18. Zhu, Q.; LeBreton, P. R. *J Am Chem Soc* 2000, 122, 12824.
19. Chen, F.; Wang, F. *Molecules* 2009, 14, 2656.
20. Hobza, P.; Havlas, Z. *Chem Rev* 2000, 100, 4253.
21. Chen, F.; Selvam, L.; Wang, F. *Chem Phys Lett* 2010, 493, 358.
22. Wang, F. *J Phys Conf Ser* 2008, 141, 012019.
23. Takahashi, M. *Bull Chem Soc Jpn* 2009, 82, 751.
24. Thom, H.; Dunning, J. *J Chem Phys* 1989, 90, 1007.
25. Wang, F.; Duffy, P.; Chong, D. P. In *Nanoscale interactions and their applications: Essays in Honour of Ian McCarthy*; Wang, F.; Brunger, M. J., Eds.; Research sign post: Kerala, India, 2007; p. 169.
26. Frisch, M. J.; Trucks, G. W.; Schlegel, H. B.; Scuseria, G. E.; Robb, M.A.; Cheeseman, J. R.; Montgomery, J. J. A.; Vreven, T.; Kudin, K. N.; Burant, J. C.; Millam, J. M.; Iyengar, S. S.; Tomasi, J.; Barone, V.; Mennucci, B.; Cossi, M.; Scalmani, G.; Rega, N.; Petersson, G. A.; Nakatsuji, H.; Hada, M.; Ehara, M.; Toyota, K.; Fukuda, R.; Hasegawa, J.; Ishida, M.; Nakajima, T.; Honda, Y.; Kitao, O.; Nakai, H.; Kelna, M.; Li, X.; Knox, J. E.; Hratchian, H. P.; Cross, J. B.; Adamo, C.; Jaramillo, J.; Gomperts, R.; Stratmann, R. E.; Yazyev, O.; Austin, A. J.; Cammi, R.; Pomelli, C.; Ochterski, J. W.; Ayala, P. Y.; Morokuma, K.; Voth, G. A.; Salvador, P.; Dannenberg, J. J.; Zakrzewski, V. G.; Dapprich, A.; Daniels, A. D.; Strain, M. C.; Farkas, O.; Malick, D. K.; Rabuck, A. D.; Raghavachari, K.; Foresman, J. B.; Ortiz, J. V.; Cui, Q.; Baboul, A. G.; Clifford, S.; Cioslowski, J.; Stefanov, B. B.; Liu, G.; Liashenko, A.; Piskorz, P.; Komaromi, I.; Martin, R. L.; Fox, D. J.; Keith, T.; Ak-Laham, M. A.; Peng, C. Y.; Nanayakkara, A.; Challacombe, M.; Gill, P. M. W.; Johnson, B.; Chen, W.; Wong, M. W.; Gonzalez, C.; Pople, J. A. *Gaussian, Inc: Wallingford, CT*, 2004.
27. Schmidt, M. W.; Baldrige, K. K.; Boatz, J. A.; Elbert, S. T.; Gordon, M. S.; Jensen, J. H.; Koseki, S.; Matsunaga, N.; Nguyen, K.A.; Su, S. J.; Windus, T. L.; Dupuis, M.; Montgomery, J. A. *J Comput Chem* 1993, 14, 1347.
28. Weigold, E.; McCarthy, I. E. *Electron Momentum Spectroscopy*; Kluwer: Dordrecht/Plenum, New York, 1999.
29. Ning, C. G.; Hajgató, B.; Huang, Y. R.; Zhang, S. F.; Liu, K.; Luo, Z. H.; Knippenberg, S.; Deng, J. K.; Deleuze, M. S. *Chem Phys* 2008, 343, 19.
30. Selvam, L.; Vasilyev, V.; Wang, F. *J Phys Chem B* 2009, 113, 11496.
31. Cederbaum, L. S. *J Phys B: At Mol Phys* 1975, 8, 290.
32. Ortiz, J. V. *J Chem Phys* 1988, 89, 6348.
33. Schipper, P. R. T.; Gritsenko, O. V.; Gisbergen, S. J. A. v.; Baerends, E. J. *Chem Phys* 2000, 112, 1344.
34. Falzon, C. T.; Wang, F.; Pang, W. *J Phys Chem B* 2006, 110, 9713.
35. Ganesan, A.; Wang, F.; Falzon, C. Intramolecular interactions of L-phenylalanine revealed by valence electronic properties of its fragments. *J Comput Chem* 2011, 32, 525.
36. Deleuze, M. S.; Trofimov, A. B.; Cederbaum, L. S. *J Chem Phys* 2001, 115, 5859.
37. Gritsenko, O. V.; Braid, B.; Baerends, E. J. *J Chem Phys* 2003, 119, 1937.
38. Powis, I.; Rennie, E. E.; Hergenbahn, U.; Kugeler, O.; Bussy-Socrate, R. *J Phys Chem A* 2003, 107, 25.
39. Wang, F. *J Phys Chem A* 2003, 107, 10199.